Journal of Alloys and Compounds 509 (2011) 2441–2444

Contents lists available at ScienceDirect

Journal of Alloys and Compounds

journal homepage: www.elsevier.com/locate/jallcom

Zinc-stearate-layered hydroxide nanohybrid material as a precursor to produce carbon nanoparticles

Mohammad Yeganeh Ghotbi [a,b,*], Narjes Bagheri [b], S.K. Sadrnezhaad [b,c]

[a] *Nanomaterials and Nanotechnology Program, Ceramic Engineering Department, Faculty of Engineering, University of Malayer, Malayer, Iran*
[b] *Materials and Energy Research Center, P.O. Box 14155-4777, Tehran, Iran*
[c] *Department of Materials Sciences and Engineering, Sharif University of Technology, P.O. Box 11365-9466, Tehran, Iran*

ARTICLE INFO

Article history:
Received 14 July 2010
Received in revised form 3 November 2010
Accepted 4 November 2010
Available online 12 November 2010

Keywords:
Nanostructured materials
Inorganic materials
Chemical synthesis
X-ray diffraction

ABSTRACT

Zinc-stearate-layered hydroxide nanohybrid was prepared using stearate anion as an organic guest, and zinc layered hydroxide nitrate, as a layered inorganic host by the ion-exchange method. Powder X-ray diffraction patterns and Fourier transform infrared results indicated that the stearate anion was actually intercalated into the interlayer of zinc layered hydroxide nitrate and confirmed the formation of the host–guest nanohybrid material. Also, surface properties data showed that the intercalation process has changed the porosity for the as-prepared nanohybrid material in comparison with that of the parent material, zinc hydroxide nitrate. The nanohybrid material was heat-treated at 600 °C under argon atmosphere. Stearate anion was chosen as a carbonaceous reservoir in the nanohybrid to produce carbon nanoparticles after heat-treating of the nanohybrid and subsequently acid washing process.

1. Introduction

Considerable attention is being focused on different types of anionic layered materials and their organic–inorganic nanohybrids, as they are considered good candidates for use in various areas of industry and medical applications [1–9]. This is due to their ability to intercalate various functional anions between their layers and other important physicochemical properties for technological applications as food additive [10] and controlled release [11] formulations, biosensor [12], ion scavenger [13–15], electrochemical performance [16], etc. Furthermore, they have frequently been used as precursors and templates to produce various metal oxides [17], catalysts [18], carbon [19], porous materials [20], etc.

Zinc layered hydroxide nitrate (ZLH) is an anionic synthetic layered material whose layers are constructed by hydroxide groups and water molecules [17]. Octahedral holes within the layers are occupied by only one type cation, zinc ions. This is against the other anionic layered materials, layered double hydroxides (LDHs) with at least two types of cations within the layers [11]. The nitrate groups are positioned between the layers freely and are not directly coordinated with the zinc ions in the ZLH [17]. The intercalation or ion-exchange process of the interlayer nitrates with other inorganic or organic anions can improve properties rather than their counterparts or it can produce new properties for the obtained nanohybrid materials [21]. Thus, due to the fact that, the layered materials, such as ZLH and its nanohybrids are suitable precursors for upcoming products, the kind of the intercalated anion between the layers may play a role in determining the properties of these materials and also the resultant products.

The aim of this study is to present the intercalation of stearate anion (SA) between zinc hydroxide nitrate layers for the formation of a new organic–inorganic nanohybrid material (ZLHSA) using simple ion-exchange method. Also, heat-treatment of the nanohybrid sample at 600 °C leads to produce carbon nanoparticles. Results from the powder X-ray diffraction (PXRD), Fourier transform infrared (FTIR), field emission scanning electron microscopy (FESEM) and also surface area studies are discussed.

2. Experimental

All solutions were prepared using de-ionized water. Zinc hydroxide nitrate was synthesized according to our previous work [17]. Briefly, in a typical experimental procedure, slow dropwise addition of 0.5 M NaOH solution into 0.2 M of $Zn(NO_3)_2$ solution with vigorous stirring under nitrogen atmosphere was done. The solution was kept at pH 7.0 (±0.05). The precipitate was filtered, washed three times with water and two times with acetone and dried in an oven overnight at 70 °C. The ZLH-stearate nanohybrid (ZLHSA) was obtained by contacting 0.5 g of the pre-prepared ZLH into 200 ml solution of 0.1 M SA (in acetone) for 2 h. The nanohybrid material, ZLHSA was heated at 600 °C in an electric tubular furnace under argon atmospheric pressure at a flow rate of 100 ml/min for 2 h at a rate of 5 °C/min and then cooled

---

* Corresponding author at: Nanomaterials and Nanotechnology Program, Ceramic Engineering Department, Faculty of Engineering, University of Malayer, Malayer, Iran. Tel.: +98 8512232346; fax: +98 8512221977.
E-mail addresses: myeganeh@malayeru.ac.ir, yeganehghotbi@gmail.com (M.Y. Ghotbi).

0925-8388/$ – see front matter © 2010 Elsevier B.V. All rights reserved.
doi:10.1016/j.jallcom.2010.11.041

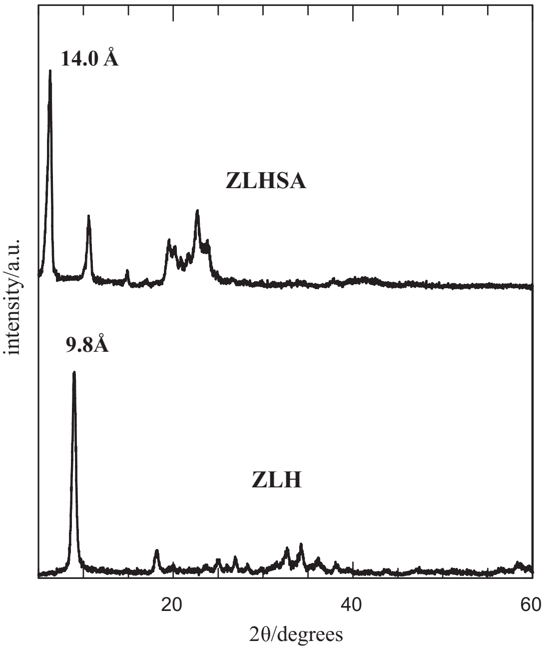

Fig. 1. PXRD patterns for zinc layered hydroxide nitrate, ZLH and its resulting nanohybrid with SA, ZLHSA.

down naturally under argon atmosphere. To obtain carbon nanoparticles, the heat-treated material was dissolved in 1 M HCl (0.5 g solid/100 ml) at 50 °C for 4 h with stirring.

Powder X-ray diffraction (PXRD) patterns were collected on a UNISANTIS XMD300 powder diffractometer unit using CuKα (λ = 1.54 Å) at 45 kV and 0.8 mA. Fourier transform infrared (FTIR) spectra were recorded using a BRUKER (VECTOR 33) spectrophotometer in the range of 400–4000 cm^{-1}. The surface area and pore size analyses were determined with a BELSORP measuring instrument (BELSORP-mini, JAPAN, INC) using nitrogen gas adsorption–desorption technique at 77 K. The carbon nanoparticles morphology was characterized by a field emission scanning electron microscopy (FESEM, JEOL JFM-6700F) together with energy-dispersive X-ray spectroscopy (EDX) that was used to determine the elemental composition of the carbon nanoparticles.

3. Results and discussion

3.1. Powder X-ray diffraction

Fig. 1 shows the powder X-ray diffraction (PXRD) patterns for the as-prepared zinc layered hydroxide nitrate, ZLH and its resulting nanohybrid with SA, ZLHSA, respectively. ZLH has a brucite-like structure with high crystallinity as shown by the narrow width of the reflection peaks, especially basal spacing with around 9.8 Å [17,19]. As shown in the figure, PXRD pattern for the nanohybrid, ZLHSA has a new sharp peak that can be observed at around 14.0 Å. This shows that the ion-exchange process of nitrate with SA was done completely, evidenced by the lack of the peak due to the parent material, ZLH at 9.8 Å. That is, nitrate was replaced by bigger size stearate anions, SA in the interlayer of the ZLH, and SA has expanded the basal spacing from 9.8 Å in the ZLH to 14.0 Å in the nanohybrid.

3.2. FTIR study

FTIR spectrum for ZLH is shown in Fig. 2a. Lattice vibrations of metal–oxygen bonds Zn–O are observed at around 467 and 436 cm^{-1} [19,22]. The band at around 634 cm^{-1} is attributed to the δ-mode of the O–H groups [17,23]. A weak peak at 840 cm^{-1} shows the υ_2 mode of the interlayer anion, nitrate in ZLH where υ_3 vibrational mode of the same anion is observed sharply at 1382 cm^{-1} [17,24,25]. At around 1635 cm^{-1} water-bending vibrations (δ_{H_2O}) of the interlayer water molecule is observed [17]. A broad band at about 3492 cm^{-1} is due to O–H groups within the layers and presence of H_2O molecules between the layers of ZLH and/or physically adsorbed water molecule stretching [17,24]. The broadness of this peak shows that the O–H groups are involved predominantly in hydrogen bonding with zinc metal hydroxide and the water molecules [10,17,24].

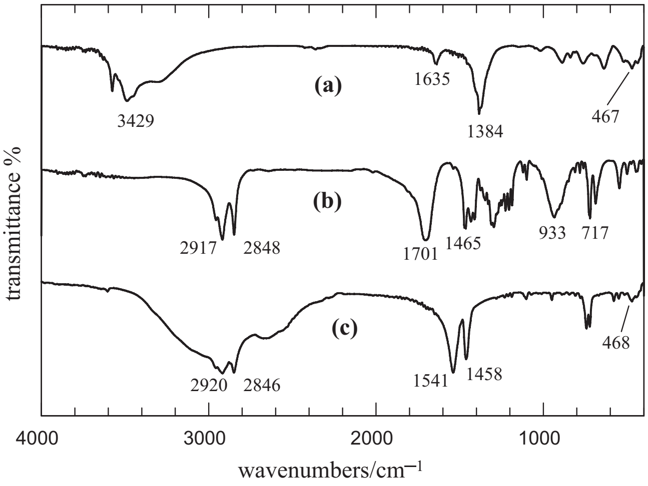

Fig. 2. FTIR spectra for the as-prepared ZLH (a), stearic acid (b) and zinc-stearate-hydroxide nanohybrid, ZLHSA (c).

The FTIR spectrum of stearic acid (Fig. 2b) shows two sharp bands at 2917 and 2848 cm^{-1}, which are due to the methylene asymmetric and symmetric C–H stretching vibrations, respectively [26,27]. As observed, the presence of carboxylic group of C=O stretching vibration is described by the presence of the band at 1701 cm^{-1} [26,27]. Methylene scissoring vibrations can be obtained by the band at 1465 cm^{-1} [27]. The band at 1296 cm^{-1} is due to methylene twisting vibrations while the one that is at around 933 cm^{-1} is attributed to C–O–H out of plane bending vibrations of the acidic group [27]. The band at around 717 cm^{-1} is due to methylene $-CH_2-$ rocking vibrations [27].

Fig. 2c shows the FTIR spectrum of ZLHSA, the as-prepared nanohybrid. As expected, the spectrum resembles a mixture of each spectrum of SA and ZLH. This means that spectral band features of both SA and ZLH are simultaneously present in the nanohybrid, ZLHSA. In addition, the C–H stretching vibration in the nanohybrid appears in the range of 2400–2800 cm^{-1}. Two bands at 2920 and 2846 cm^{-1} are assigned to the methylene C–H stretching vibrations. A broad absorption band at around 3000 cm^{-1} combined with the methylene C–H stretching vibrations is attributed to the O–H stretching due to the presence of hydroxyl group in ZLH, indicating the presence of the hydrogen bond between the layers [10,19]. The carboxylate group gives rise to a band at 1541 cm^{-1}. Shifting of the band as compared to that of free stearic acid reveals that hydrogen bonding in the intercalated SA with hydroxyl groups within the brucite-like layers and the intercalated water molecules is much stronger than that for free stearic acid [11,19,28]. Bands at around 1458 cm^{-1} is due to $-CH_2-$ scissoring vibration, at 725 cm^{-1} is attributed to methylene rocking vibrations, and at around 468 cm^{-1} is associated with the M–O of the host material, ZLH.

3.3. Surface properties study of ZLH and ZLHSA

Adsorption–desorption isotherms of nitrogen gas on ZLH and its nanohybrid with SA, ZLHSA and their pore size distributions are given in Fig. 3. Also, surface properties data are summarized in Table 1. Brunauer–Emmett–Teller (BET) surface area values of ZLH and its nanohybrid with SA intercalated between the layers

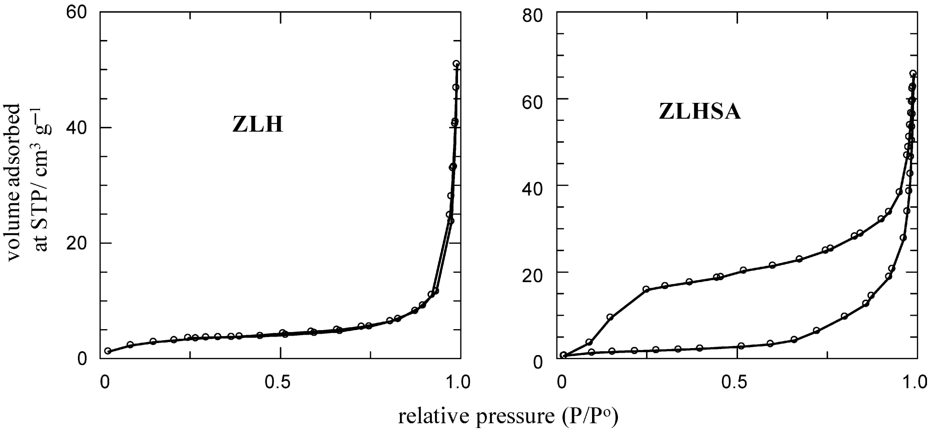

Fig. 3. Adsorption–desorption isotherms of nitrogen gas for zinc layered hydroxide nitrate, ZLH and its resulting nanohybrid with SA, ZLHSA.

Table 1
Obtained data from surface analyses of ZLH and its nanohybrid with SA, ZLHSA.

Sample	Surface area[a] (m^2/g)	Total pore volume[a], V_t (cm^3/g)	Average pore diameter[a] (nm)	BJH $r_{p,\ peak}$ (nm)
ZLH	10	0.07	27	14.13
ZLHSA	10	0.11	62	1.85

[a] Calculated by BET method.

are both the same and around $10\,m^2 g^{-1}$. On the contrary, total pore volume for ZLH is $0.077\,cm^3\,g^{-1}$ and this has increased to $0.10\,cm^3\,g^{-1}$ when SA anion was intercalated between the layers of ZLH to replace the nitrate and to obtain the nanohybrid, ZLHSA. The Barret–Joyner–Halenda (BJH) pore size distributions for ZLH and ZLHSA show that they are of the mesoporous-type materials [17,29]. However, the pore size distribution for ZLH shows a sharp peak centered at around 14.13 nm and a few small single-peaks while for ZLHSA only one single-peak pore size distribution at around 1.85 nm is observed (Fig. 4). In general, the pore size distributions show the formation of more regular mesopores in the ZLHSA compared to that of the parent material, ZLH. The adsorption–desorption isotherms for both ZAL and ZLHSA belong to Type II which is characteristic of a plate-like material. ZLH almost does not show hysteresis where ZLHSA depicts fat Type H3 hysteresis loop indicating of slit-shaped pores [29].

3.4. Surface morphology study of carbon nanoparticles

The morphology of the carbon nanoparticles obtained from the heat-treated nanohybrid, ZLHSA at 600 °C and subsequent acid washing process was studied with FESEM as illustrated in Fig. 5.

Fig. 5. Surface morphology of carbon nanoparticles obtained from heating of ZLHSA at 600 °C after acid washing process.

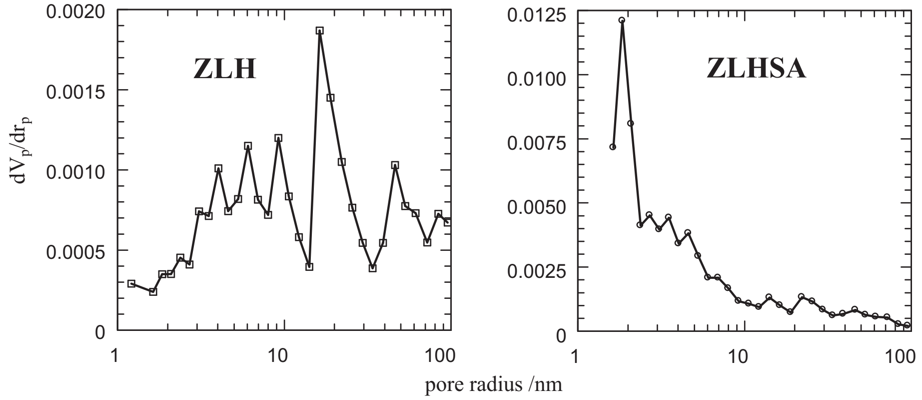

Fig. 4. BJH desorption pore size distributions for zinc layered hydroxide nitrate, ZLH and its resulting nanohybrid with SA, ZLHSA.

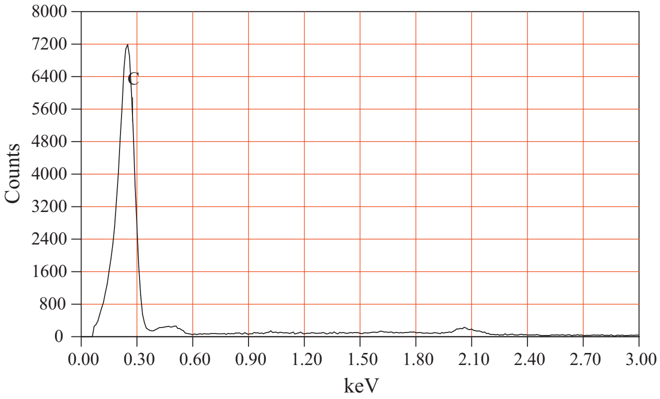

Fig. 6. Energy-dispersive X-ray spectroscopy (EDX) of carbon nanoparticles obtained from heating of ZLHSA at 600 °C after acid washing process.

The image clearly shows the plates with rough surface which are smaller than 100 nm. EDX analysis confirmed the presence of 100% carbon material without any impurity in the carbon nanoparticles after acid washing process as shown in Fig. 6.

4. Conclusions

Carbon nanoparticles can be obtained by the heat-treatment of an easy to make layered nanohybrid material, zinc-stearate-layered hydroxide. This new organic-clay nanohybrid material, in which the organic moiety is intercalated between the inorganic layers, was synthesized using stearate anion as a guest and zinc hydroxide nitrate as an inorganic layered host by ion-exchange technique. In comparison with other methods such as CVD where the organometallic precursors are pricy and laser ablation in which the products are in low quantities and the utilized apparatuses are expensive, the proposed method is very simple, the chemicals used in the synthesis are cheap and the manner is economical and suitable for a large scale production of nano-sized carbon nanoparticles.

Acknowledgement

The authors would like to thank Material and Energy Research Center (MERC), for supporting this work.

References

[1] Z.P. Xu, P.S. Braterman, Appl. Clay Sci. 48 (2010) 235–242.
[2] Y. Shi, F. Chen, J. Yang, M. Zhong, Appl. Clay Sci. 50 (2010) 87–91.
[3] D. Pan, H. Zhang, T. Zhang, X. Duan, Chem. Eng. Sci. 65 (2010) 3762–3771.
[4] R. Marangoni, A. Mikowski, F. Wypych, J. Colloid Interface Sci. 351 (2010) 384–391.
[5] G.S. Machado, G.G.C. Arízaga, F. Wypych, S. Nakagaki, J. Catal. 274 (2010) 130–141.
[6] F. Kovanda, E. Jindová, K. Lang, P. Kubát, Z. Sedláková, Appl. Clay Sci. 48 (2010) 260–270.
[7] X. Kong, L. Jin, M. Wei, X. Duan, Appl. Clay Sci. 49 (2010) 324–329.
[8] R.M. Borges, G.G.C. Arizaga, F. Wypych, Biochem. Eng. J. 48 (2009) 93–98.
[9] T. Kijima, T. Isayama, M. Sekita, M. Uota, G. Sakai, J. Alloys Compd. 485 (2009) 730–733.
[10] M.Y. Ghotbi, M.Z.b. Hussein, A.H. Yahaya, M.Z.A. Rahman, J. Phys. Chem. Solids 70 (2009) 948–954.
[11] M. Yeganeh Ghotbi, M.Z.b. Hussein, J. Phys. Chem. Solids 71 (2010) 1565–1570.
[12] M.S.P. Lopez, F. Leroux, C. Mousty, Sens. Actuators B: Chem. 150 (2010) 36–42.
[13] T. Kameda, T. Yamazaki, T. Yoshioka, Mater. Res. Bull. 45 (2010) 751–753.
[14] R. Chitrakar, S. Tezuka, J. Hosokawa, Y. Makita, A. Sonoda, K. Ooi, T. Hirotsu, J. Colloid Interface Sci. 349 (2010) 314–320.
[15] T. Kameda, T. Yamazaki, T. Yoshioka, Solid State Sci. 12 (2010) 946–951.
[16] A.B. Béléké, M. Mizuhata, J. Power Sources 195 (2010) 7669–7676.
[17] M.Z.b. Hussein, M.Y. Ghotbi, A.H. Yahaya, M.Z. Abd Rahman, Solid State Sci. 11 (2009) 368–375.
[18] H. Liu, Q. Jiao, Y. Zhao, H. Li, C. Sun, X. Li, J. Alloys Compd. 496 (2010) 317–323.
[19] M.Y. Ghotbi, M.Z.b. Hussein, A.H. Yahaya, M.Z. Abd Rahman, Solid State Sci. 11 (2009) 2125–2132.
[20] J. Zhu, Z. Gui, Mater. Chem. Phys. 118 (2009) 243–248.
[21] G.G.C. Arizaga, K.G. Satyanarayana, F. Wypych, Solid State Ionics 178 (2007) 1143–1162.
[22] M.Y. Ghotbi, J. Alloys Compd. 491 (2010) 420–422.
[23] Z.P. Xu, H.C. Zeng, Chem. Mater. 13 (2001) 4555–4563.
[24] M.Z.b. Hussein, M.Y. Ghotbi, A.H. Yahaya, M.Z. Abd Rahman, Mater. Chem. Phys. 113 (2009) 491–496.
[25] F. Wypych, G. Guadalupe Carbajal Arizaga, J.E. Ferreira da Costa Gardolinski, J. Colloid Interface Sci. 283 (2005) 130–138.
[26] B. Stuart, Infrared Spectroscopy: Fundamentals and Applications, John Wiley & Sons, Ltd., Chichester, 2004.
[27] D. Li, L. Wang, D. Xue, J. Alloys Compd. 492 (2010) 564–569.
[28] Y. Feng, D. Li, Y. Wang, D.G. Evans, X. Duan, Polymer Degrad. Stabil. 91 (2006) 789–794.
[29] K.S.W. Sing, D.H. Everett, R.A.W. Haul, L. Moscou, R.A. Pierotti, J. Rouquerol, T. Siemieniewska, Pure Appl. Chem. 57 (1985) 603–619.